DYNA
http://dyna.medellin.unal.edu.co/

UNIVERSIDAD NACIONAL DE COLOMBIA

Macroscopic and population balances for the simulation of surface reactions

Carolina Cruz & Daniel Barragán

Universidad Nacional de Colombia, sede Medellín, Facultad de Ciencias, Medellín, Colombia. cacruzca4@gmail.com, dalbarraganr@unal.edu.co

Received: March 10th, 2022. Received in revised form: September 15th, 2022. Accepted: October 12th, 2022.

Abstract
Modeling and computational simulation of the carbon monoxide oxidation process, taken as a key system to analyze the importance of the dynamic description of active sites into the process yield, are presented in this work. To this aim, the formalism of transport phenomena and population balances are used to implement a realistic model that involves heat exchange, transfer of mass and momentum, chemical reaction, and catalyst deactivation. The model is solved numerically, and the analysis is made by comparing isothermal pseudo-steady state approximation with non-isothermal non-steady state assumption for the catalytic cycle. The results show the advantage of considering the interface explicitly into the model since temporary changes of the reactive complex as well as the active sites of the catalyst have a great influence over the reaction yield. By considering this fact, the reaction description is made in a more proper way.

Keywords: transport phenomena; population balances; kinetic cycle; surface catalyst.

Balances macroscópicos y poblacionales para la simulación de reacciones en la superficie

Resumen
En este trabajo presentamos el modelamiento y simulación computacional de la oxidación del monóxido de carbono, proceso que tomamos como referente para analizar la importancia de describir la dinámica de los sitios activos en el rendimiento del proceso catalítico. Utilizamos el formalismo de los procesos de transporte y los balances poblaciones para desarrollar un modelo realístico que involucra el intercambio de calor, la transferencia de masa y de momentum, la reacción química y la desactivación del catalizador. El modelo propuesto se resuelve numéricamente y se hace un análisis comparativo de los resultados entre la aproximación de pseudo estado estacionario isotérmico y el estado no-estacionario no-isotérmico para el ciclo catalítico. Los resultados obtenidos muestran la importancia de considerar en el modelo la interfase de manera explícita, ya que la dinámica temporal de la reacción y de los sitios activos influyen de manera significativa en el rendimiento del proceso catalítico.

Palabras clave: fenómenos de transporte; balances de población; ciclo cinético; superficie de catalizador.

1 Introduction

A catalytic process can be analyzed from a set of perspectives, such as a purely chemical kinetic approach, macroscopic balances of matter and energy, chemical master equation, and population balances. The implementation of one approach depends on the kind of available data and on what type of information it is expected to obtain about the system. In many cases, using more than one approach would be advisable [1-3]. Due to the vast implementation of heterogeneous catalytic-based processes, there is a great interest in understanding them through mathematical modeling and simulations.

The derivations of kinetic expressions for catalytic cycles constitute a well-developed area in the context of chemical catalysis. However, works performed in this field do not include the influence of the transitions states or reactive intermediates [4]. Moreover, additional processes should be considered to analyze the changes of catalyst properties under reaction conditions. For instance, one of the components can diffuse into the subsurface layers of metallic catalyst, causing surface modification [5].

How to cite: Cruz, C. and Barragán, D., Macroscopic and population balances for the simulation of surface reactions. DYNA, 89(224), pp. 66-75, October - December, 2022.

Kozuch and Shaik [4] proposed a combined kinetic-quantum chemical model to estimate the overall net rate of a catalytic cycle called *turnover frequency* (TOF) in terms of the energetics of its individual steps; furthermore, this procedure allows a straightforward estimation of the cycle efficiency by computational means. Although this initiative to analyze the cycle performed by the catalyst represents significant progress, it is necessary further studies that lead to a deeper understanding of the phenomenon of catalysis [6].

Heterogeneous catalysis is a complex multiscale process. On the macroscopic scale, computational simulations based on continuum theories (such as the Navier–Stokes equations) are the most widely used approach to describe heat and mass transport [7]. However, with particulate processes, an additional balance is required to describe how the particle population changes during the process. In general, particulate systems are more difficult to describe than systems comprised of one or more bulk phases [8,9]. Population balances are frequently used to describe and control many-particulate processes such as crystallization, granulation, flocculation, combustion, polymerization, and catalysts deactivation [10]. According to [11], "the catalytic process is a sequence of elementary steps that form a cycle from which the catalyst emerges unaltered". However, it is known that the kinetic cycle performed by the catalyst is irreversible by nature, meaning that there is a partial reconstruction of the catalyst before the next cycle begins [12]. This fact influences the global performance of the process. Population balances reveal that, after a chemical reaction, the catalyst does not return to its initial state because there are chemical or physical processes happening simultaneously with the main reaction causing the catalyst deactivation, which is understood as the loss of catalyst activity since there are fewer active sites in each cycle.

This work aims to understand and describe a generic heterogeneous catalytic reaction by implementing two complementary approaches. Thus, the paper is organized as follows. In *section 2.1*, we describe the system under consideration which is composed of two subsystems. In *section 2.2*, we propose macroscopic balances for each subsystem based on the specific phenomena that take place in each of them. In *section 2.3*, we implement population balances to describe the temporal evolution of a population of particles, that is, the number of active sites of the catalyst. After deriving a generic model, in *section 2.4*, we introduce a case study corresponding to the catalytic oxidation of carbon monoxide. In *section 3*, we present the results and discussion of the case study. In *section 3.1*, we assume isothermal and pseudo-steady state conditions; in *section 3.2*, we consider a non-isothermal reaction-diffusion system; finally, we study catalyst deactivation in *section 3.3*. *Section 4* corresponds to the conclusions.

2 The model

2.1 The system

Fig. 1 represents a generic heterogeneous catalytic system. In the diagram presented on the left-side, there is a gas stream crossing over the catalyst where δ corresponds to the height of the gas film and σ is the interface that separates phases α and β. While the gas is flowing, the reactants are adsorbed onto the catalyst and react to form the product. The chemical reaction occurs at the gas-solid interface. It is important to note that the gas phase and catalyst are coupled systems, exchanging mass and energy. There is no chemical reaction in the gas phase, but there are diffusion and convection. It is assumed that convection is a one-dimensional phenomenon over x axis while diffusion occurs over x and y axis. The gas is not confined; hence there is no hydrodynamic pressure gradient, and instead of that, there is a pressure gradient due to concentration changes. On the other hand, there is no convection in the catalyst. The chemical reaction is carried out across the x axis, and diffusion is a two-dimensional phenomenon.

The presence of an interface influences all thermodynamic parameters of the system. According to Gibbs's description, both phases α and β are separated by an infinitesimal thin boundary layer called Gibbs dividing plane or ideal interface. In this model, an interface is an imaginary plane placed at an arbitrary position parallel to the phases [13]. In the idealized system, the chemical compositions of phases α and β are assumed to remain unchanged right up to the imaginary dividing surface.

The study of systems involving multi-component mass transfer to\from a catalytic surface is made employing the film model. However, in the frame of this model, some questionable assumptions are made. First, it is assumed that the temperature and chemical potentials of the surface are equal to those in the adjacent homogeneous region. Second, coupling effects between mass and heat fluxes are neglected [14,15].

The interface is explicitly considered a system in the description to propose a realistic model and not just to establish boundary conditions. Fig. 1(right-side) corresponds to a schematic diagram of the temperature variation in the heterogeneous exothermic catalytic reaction. This variation

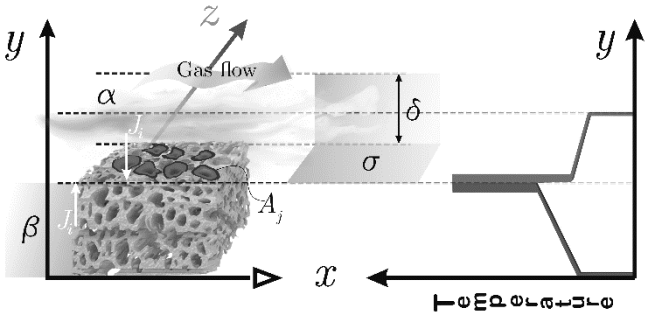

Figure 1. (left-side) Gibbs ideal interface where phases α, and β, are separated by a plane σ which corresponds to the interface. (right-side) Schematic diagram of temperature variations in a heterogeneous catalytic system. Adapted from [14]. The catalyst temperature differs from the adjacent homogeneous phase due to the exothermic reaction, and it is assumed to be constant at the surface. In the left-side scheme, the active zones area is assumed to decrease. The catalyst surface has some active zones of area A_j. The zones in dark gray have smaller areas since, after the chemical reaction, there is incomplete desorption of the chemical species. Additionally, the reactants flow is a mixture of CO, CO_2, O_2 and inerts. The latter acts as a poison. Inert compounds do not react but can occupy a fraction of the active zones, thus reducing their area.
Source: Own elaboration.

has been demonstrated experimentally [15,16] and theoretically [16,17]. In this diagram, the catalyst temperature differs from the adjacent phase, and the temperature on both sides of the surface may differ; in addition, it is assumed that the catalyst temperature is uniform over the surface [18].

2.2 Macroscopic balances

If the temperature or the concentrations of chemical species in a system are perturbed, then they become nonuniform, and their respective gradients appear and vanish over time [18,19].

The basic form of the conservation equation for specie i is given by the following expression [20]:

$$\frac{\partial C_i}{dt} = -\nabla \cdot \mathbf{N_i} + \nu_i \tag{1}$$

The source term ν_i is the net formation rate of specie i by chemical reactions per unit volume. The sign convention is such the rate is positive if there is the net formation of species i, and negative if there is net consumption. The rates of heterogeneous reactions appear only in interfacial conditions. In addition, C_i is the molar concentration of the specie i (in units of mol/m^3). The total molar flux $\mathbf{N_i}$ involves the convective and diffusive fluxes of species i:

$$\mathbf{N_i} = C_i\mathbf{v} + \mathbf{J_i} \tag{2}$$

The first term in Equation (2) corresponds to the convective flux and the second term is the diffusive flux with $\mathbf{J_i}$ being the molar flux of specie i relative to the mass-average velocity, $\mathbf{v}$. When density and diffusivity are constant, the conservation equations for species i can be written as:

$$\frac{\mathrm{DC_i}}{\mathrm{Dt}} = \mathrm{D_i}\nabla^2\mathrm{C_i} + \nu_\mathrm{i} \tag{3}$$

where the differential operator, D/Dt is the material or substantial derivative. Alternatively, Equation (1) can be expressed in rectangular coordinates as follows:

$$\frac{\partial C_i}{\partial t} + \upsilon_x\frac{\partial C_i}{\partial x} + \upsilon_y\frac{\partial C_i}{\partial y} + \upsilon_z\frac{\partial C_i}{\partial z} = D_i\left[\frac{\partial^2 C_i}{\partial x^2} + \frac{\partial^2 C_i}{\partial y^2} + \frac{\partial^2 C_i}{\partial z^2}\right] + \nu_i \tag{4}$$

Specifically, in the bulk phase, there is no reaction, but there is convection over x-direction and diffusion over y-direction (see Fig. 1(left-side)). In this case, the mass transfer occurs in two dimensions. To reduce the problem's complexity, we made an average over the y-axis by integrating Equation (4) with respect y between 0 and δ. A parabolic form of the diffusion term is obtained, and it is assumed that the diffusion across the y-axis is given by the net adsorption rate of the species. The expression for conservation of mass of specie i is:

$$\frac{\partial C_i}{\partial t} + \delta\upsilon_x\frac{\partial C_i}{\partial x} = D_i\left[\delta\frac{\partial^2 C_i}{\partial x^2}\right] + J_y \tag{5}$$

where J_y is an average diffusive flux over y-direction and corresponds to the net velocity of adsorption and desorption, $J_y \approx \upsilon_{ads} + \upsilon_{des}$, being υ_{ads} the adsorption rate and υ_{des} the desorption rate. These quantities depend on the reaction mechanism. The second term on the left-hand side of Equation (5) is the convective contribution in the mass balance, and the first term on the right hand is the diffusive term, both in x -direction.

In the catalyst, there is no convection, but reaction and diffusion occur in two dimensions. Like done in the previous case, an average diffusive flux is calculated by integrating Equation (4) with respect to y. Then, if the diffusion across y-axis is given by a net adsorption-desorption rate of the species i, the conservation of mass of adsorbed species j is given by:

$$\frac{\partial C_j}{\partial t} = D_j\left[\delta\frac{\partial^2 \mathrm{C_j}}{\partial x^2}\right] - J_y + \delta\nu_j \tag{6}$$

Note that in Equation (6), there is no convective contribution; instead, there are diffusive terms: the first and second terms on the right hand of the equation, and the source term contribution, ν_j due to the chemical reaction at the interface. Moreover, recalling the catalyst is another study system then, a dynamic balance of the number of active sites per volume of catalyst, Ψ, is made as follows:

$$\delta\frac{\partial \Psi}{\partial t} = D_Z\left[\delta\frac{\partial^2 \Psi}{\partial x^2}\right] - J_y + \delta\nu_Z \tag{7}$$

where the subscript Z indicates an active site in the catalyst. Note again that the first and second terms on the right-hand side of Equation (7) are the diffusive contributions, and the last term accounts for the chemical reaction.

On the other hand, the general form of the multi-component energy equation in terms of partial molar enthalpies $\bar{H}_i$ is:

$$\frac{\partial}{\partial t}\left(\sum_{i=1}^{n} C_i\bar{H}_i\right) = -\nabla\cdot\mathbf{e} + \frac{DP}{Dt} + \boldsymbol{\tau}\colon\nabla\mathbf{v} + \sum_{i=1}^{n}\mathbf{j_i}\cdot g_i \tag{8}$$

The partial molar enthalpy is defined as follows:

$$\bar{H}_i = C_{p,i}\left(T - T_{ref}\right) \tag{9}$$

where $T_{ref} = 298.15K$ and $C_{p,i}$ is the heat capacity of species i. Replacing Equation (9) into Equation (8) and neglecting pressure, viscous, and Dufour effects, the following expression for the energy conservation is obtained:

$$\left(\sum_{i=1}^{n} C_{p,i} C_i \frac{\partial T}{\partial t}\right) = -\nabla \cdot \mathbf{e} - \left(T - T_{ref}\right) \sum_{i=1}^{n} C_{p,i} \frac{\partial C_i}{\partial t} + \sum_{j=1}^{m} \nu_j \Delta H_j + q \tag{10}$$

It is important to note that the last two terms on the right-hand side of Equation (8) were not included in the previous deduction. However, the terms $\sum_{j=1}^{m} \nu_j \Delta H_j$ is related to the energy transfer due to the chemical reactions and q is the transferred heat between phases which is defined by an expression analogous to Newton's cooling law [20,21]:

$$q = U(T - T_{cat}) \tag{11}$$

where U is the global heat transfer coefficient per unit area of the catalyst, and T_{cat} is the catalyst temperature.

Finally, the general expression of conservation of linear momentum is written as:

$$\rho \frac{D\upsilon}{Dt} = \rho \mathbf{g} - \nabla P + \mu \nabla \cdot \boldsymbol{\tau} \tag{12}$$

where ρ is the density of the mixture and μ is the viscosity. In rectangular coordinates along the x axis:

$$\rho \left[\frac{\partial \upsilon_x}{\partial t} + \upsilon_x \frac{\partial \upsilon_x}{\partial x}\right] = -\frac{\partial P}{\partial x} + \mu \left[\frac{\partial \tau_{xx}}{\partial x} + \frac{\partial \tau_{xy}}{\partial y}\right] \tag{13}$$

Viscous stresses, τ_{ij} are given by the following expressions:

$$\tau_{xx} = 2\mu \left[\frac{\partial \upsilon_x}{\partial x} - \frac{1}{3} \nabla \cdot \mathbf{v}\right] \tag{14}$$

$$\tau_{xy} = \mu \left[\frac{\partial \upsilon_x}{\partial y} + \frac{\partial \upsilon_y}{\partial x}\right] \tag{15}$$

With

$$\nabla \cdot \mathbf{v} = \frac{\partial \upsilon_x}{\partial x} + \frac{\partial \upsilon_y}{\partial y} + \frac{\partial \upsilon_z}{\partial z} \tag{16}$$

The goal is to calculate the velocity variation over time, but it is important to note that velocity is a function of two spatial coordinates: $\upsilon_x = \upsilon_x(x, y)$, however for the sake of simplicity, it is possible to assume that velocity changes only depend on the x-coordinate and taking an average over y-axis, the velocity is given by Stokes flow:

$$\upsilon_x(y) = \frac{\Delta P}{L}\left(1 - \left(\frac{y}{\delta}\right)^2\right) \tag{17}$$

Integrating Equation (17) with respect to y between 0 and δ, the average velocity on y-coordinate is obtained:

$$\langle \upsilon_x \rangle = \frac{\Delta P}{L} \int_0^L \left(1 - \left(\frac{y}{\delta}\right)^2\right) dy \tag{18}$$

Equation (18) is solved to calculate the velocity changes over time, and it is valid only for the bulk phase. On the other hand, a pressure gradient is associated with concentration changes. In this case, the ideal gas model was used

$$\frac{\partial P}{\partial x} = \sum_{i=1}^{N} C_i R \frac{\partial T}{\partial x} \tag{19}$$

2.3 Population balances

The population balance equation accounts for the various ways in which particles of a specific state can either form or disappear from the system [9,22-24]. A population balance for particles in some fixed subregion of particle phase space is given by the balance *(accumulation)=(input)-(output)+(net generation)*.

Consider a given subregion R_1 that is moving with the particle phase-space velocity $\mathbf{v}$, then the population balance for particles in R_1 is given by:

$$\frac{d}{dt} \int_{R_1} n \, dR = \int_{R_1} (B - D) dR \tag{20}$$

The term on the left-hand of Equation (20) can be expanded using Leibnitz's rule as follows:

$$\frac{d}{dt} \int_{R_1} n \, dR = \int_{R_1} \frac{\partial n}{\partial t} \, dR + \left(n \frac{d\mathbf{x}}{dt}\right)_{R_1} = \int_{R_1} \left[\frac{\partial n}{\partial t} + \nabla \cdot \left(\frac{d\mathbf{x}}{dt} n\right)\right] dR \tag{21}$$

where $\mathbf{x}$ is the set of internal and external coordinates comprising the phase space R. Recalling that

$$\frac{d\mathbf{x}}{dt} = \mathbf{v} = \mathbf{v_e} + \mathbf{v_i} \tag{22}$$

The population balance can be written for the region R_1 as follows:

$$\int_{R_1} \left[\frac{\partial n}{\partial t} + \nabla \cdot (\mathbf{v_e} \, n) + \nabla \cdot (\mathbf{v_i} \, n) + \mathrm{D} - \mathrm{B}\right] dR = 0 \tag{23}$$

As the region R_1 is arbitrary then, the integral must vanish identically. Therefore, Equation (23) is written as:

$$\frac{\partial n}{\partial t} + \nabla \cdot (\mathbf{v} n) + \mathrm{D} - \mathrm{B} = 0 \tag{24}$$

By expanding Equation (24) in terms of the $m + 3$ coordinates, the population balance becomes [8,22]:

$$\frac{\partial n}{\partial t} + \frac{\partial}{\partial x}(\upsilon_x n) + \frac{\partial}{\partial y}\left((\upsilon_y n)\right) + \frac{\partial}{\partial z}\left((\upsilon_z n)\right) + \sum_{j=1}^{m} \frac{\partial}{(\partial x_i)_j}\left[(\upsilon_i)_j n\right] - \mathrm{B} + \mathrm{D} = 0 \tag{25}$$

The term which depends on v_i is known as the *growth rate*, whereas the terms that are a function of the external velocities: v_x, v_y and v_z denotes the *velocity*. Equation (25) is a number continuity equation in particle phase space, is entirely general, and is used when the particles are distributed along both the external and internal coordinate space. This expression must, in any case, be adapted for a particular problem [10].

Since the catalyst activity is related to the population of the available active sites [23], the catalyst deactivation process can be considered to decrease the number of available active sites at the catalyst surface. In this sense, population balance equations are a valuable tool for analyzing the loss of catalyst activity since an internal coordinate can describe the active sites. It is assumed that over the catalyst surface, many active sites are grouped in "active zones" of area A_j (see Fig. 1). Catalyst deactivation occurs because the area of the active zones is decreasing over time.

2.4 Application case

We study the catalytic oxidation of carbon monoxide. Such reaction is typical when understanding the concepts of heterogeneous catalysis (see Fig. 2) and is one of the key reactions in cleaning automotive exhaust. This process occurs in car engines to reduce emissions of toxic gases, which are products of incomplete combustion of fuels [24,25].

To describe the process, we assume that the metal surface consists of active sites, denoted as Z. The catalytic reaction cycle begins with the adsorption of CO (A) and O_2 (B) on the surface of platinum, where molecules of O_2 dissociate into two oxygen atoms:

$$A + Z \rightleftharpoons ZA$$

$$B + Z \longrightarrow 2ZB$$

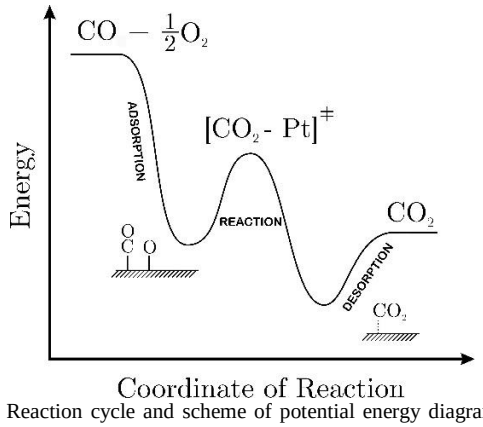

Figure 2. Reaction cycle and scheme of potential energy diagram for the catalytic oxidation of CO. Adapted from [11]. The catalytic oxidation of CO is described according to the Langmuir-Hinshelwood mechanism, molecules of O_2 are chemisorbed onto the catalyst surface, whereas CO molecules are physisorbed. Once the reactant molecules are adsorbed, they react to produce adsorbed CO_2, the cycle finishes when the product is desorbed, and the catalyst returns to its initial state. Source: Own elaboration.

The components ZA and ZB correspond to adsorbed complex, *i.e.*, atom or molecule bounded to the site Z. The adsorbed oxygen atom and the adsorbed carbon monoxide molecule then react on the surface to form CO_2 (C), which interacts only weakly with the platinum surface and is desorbed almost instantaneously [26]:

$$ZA + ZB \rightleftharpoons 2Z + C$$

Fig. 2 shows the reaction cycle and the potential energy diagram sketch. From the Langmuir-Hinshelwood mechanism, it is known that there are two steps of adsorption (v_1 and v_2) and one of reaction (v_r). The law of mass action gives the molar rates:

$$v_1 = k_1 C_A \Psi - k_{-1} C_{AZ} \tag{26}$$

$$v_2 = k_2 C_B \Psi^2 - k_{-2} C^2{}_{BZ} \tag{27}$$

$$v_r = k_f C_{AZ} C_{BZ} - k_b C_C \Psi^2 \tag{28}$$

where k_i is a reaction constant and C_j is the concentration of the specie i, Ψ is the number of active sites per volume of catalyst. The Arrhenius expression gives these reaction constants: $k_i = k_{i,0} e^{-\left(E_a/RT\right)}$, where $k_{i,0}$ is a pre-exponential factor and E_a is the activation energy in kJ/mol.

The forward kinetic constants that are used in this work are given by Rawlins et al. [27], and the backward constants are proposed to be fractions of the forward constants: $k_1 = 1.85 \cdot 10^8 \sqrt{T} e^{-(92600/1.987T)}$; $k_{-1} = 0.01 k_1$; $k_2 = 1.85 \cdot 10^8 \sqrt{T} e^{-(92600/1.987T)}$; $k_{-2} = 1.00 \cdot 10^{-4} k_2$; $k_f = 3.40 \cdot 10^7 e^{-(23400/1.987T)}$; $k_b = 0.01 k_f$.

To analyze the catalyst deactivation, consider a fraction of a surface catalyst with active zones, as shown in Fig. 1. It is assumed that the reactants flow is a mixture of CO, O_2, CO_2 and inert compounds, specifically sulphur (S) and carbon (E), which do not participate in the chemical reaction but can be adsorbed into the active sites and prevent the reactants from being adsorbed. Thereby, inert compounds block the active sites and reduce the active zones area. Additionally, it is assumed that, after the chemical reaction, the desorption of the species is incomplete, *i.e.*, a portion of the product and the reactants remain adsorbed, and hence, there is a decrease in the area of the active zones. Thus, to account for this phenomenon, besides the main steps of the carbon monoxide oxidation mechanism over a platinum catalyst, an additional reaction step to describe catalyst deactivation by poisoning and coking is considered, as follows:

$$2ZA \rightleftharpoons ZE + CO_2 + Z$$

$$Z + S \rightleftharpoons ZS$$

These reaction steps correspond to the coking and poisoning processes, respectively. To deduce the population balance equation is necessary to determine the internal

coordinate. In this case, it is convenient to choose the active zones area A as the internal coordinate. Therefore, the general form of the population balance (see Equation (25)) is given by:

$$\frac{\partial n}{\partial t}+\frac{\partial}{\partial x}(v_x n)+\frac{\partial}{\partial y}\left((v_y n)\right)+\frac{\partial}{\partial z}\left((v_z n)\right) + \frac{\partial}{\partial A}\left[\left(\frac{\partial A}{\partial t}\right)n\right]-\mathrm{B}+\mathrm{D}=0 \tag{29}$$

where A corresponds to the area (in nm^2) of the active zones, and B and D are the terms of birth and death, respectively. We assume that the active zones will not appear or disappear. Thus, the birth and death terms are negligible. Furthermore, the active zones are not moving over the catalyst surface, meaning that $v_x = v_y = v_z = 0$. For the study case, only the time derivative of the internal coordinate (area of active zones) is considered, and Equation (29) can be rewritten as:

$$\frac{\partial n}{\partial t}-\frac{\partial}{\partial A}\left[\left(\frac{\partial A}{\partial t}\right)n\right]=0 \tag{30}$$

Equation (30) is solved using the Moments Method [28–30], which is defined, for this study system, as:

$$n(A,x,t)dA \quad \equiv \quad \text{Number of active sites having area within the range between } A \text{ and } A+dA$$

$$M_0=\int_0^\infty n(A,x,t)dA \quad \equiv \quad \text{Number of available active sites}$$

$$M_1=\int_0^\infty An(A,x,t)dA \quad \equiv \quad \text{Total active area}$$

where x represents the spatial coordinate and t is time. Moreover, using this method, a mean area of the active zone (average active area) can be defined as follows:

$$\langle A\rangle=\frac{M_1}{M_0}=\mu \tag{31}$$

The temporary change of the average active area can be defined as a function of the rates of each mechanism step. In other words, the temporary change of the internal variable depends on the rate of adsorption, desorption, reaction, poisoning, and coking. Thus, we write the following expression:

$$\langle\frac{\partial A}{\partial t}\rangle=\nu_1+\nu_2+\nu_r+\nu_{poison}+\nu_{coke} \tag{32}$$

where ν_i is the rate of the i step of the reaction mechanism, where:

$$\nu_{poison}=-k_{+c}C_{ZA}+k_{-c}C_C\Psi C_E \tag{33}$$

$$\nu_{coke}=-k_{+p}\Psi C_S+k_{-p}C_{ZS} \tag{34}$$

The terms ν_i, B and D are assumed negligible since the active zones are stationary. Moreover, neither the active sites are created nor disappear, but the active zones' area decreases. The temporary changes of moments are given by:

$$\frac{\partial M_0}{\partial t}=0 \tag{35}$$

$$\frac{\partial M_1}{\partial t}=(\nu_1+\nu_2+\nu_{poison})M_1+(\nu_r+\nu_{coke})M_0 \tag{36}$$

$$\frac{\partial M_2}{\partial t}=(\nu_1+\nu_2+\nu_{poison})M_2+(\nu_r+\nu_{coke})M_1 \tag{37}$$

Note that M_0 is conserved because there is no birth or death of active sites. Irreversible or reversible mechanisms are considered when studying poisoning and coking processes over the catalyst activity. According to ν_{coke} and ν_{poison}, for each mechanism, there are two specific rate constants: k_+ and k_-, if the process is considered irreversible, then $k_- \approx 0$.

Finally, by assuming a normal distribution, the probability density function (PDF) is given by:

$$n(x)=\frac{1}{\varrho\sqrt{2\pi}}exp\left[-\frac{1}{2}\left(\frac{x-\mu}{\varrho}\right)^2\right] \tag{38}$$

where μ and ϱ are calculated as follows:

$$\mu=\frac{M_1}{M_0}\ ;\ \varrho=\sqrt{\left(\frac{M_2}{M_0}-\mu^2\right)}$$

3 Results and discussion

Once the study system is well described, balances of energy, mass, momentum, and population are solved to analyze the dynamic behavior of this catalytic reaction. The analysis is made under different scenarios, and the results are shown below.

3.1 Pseudo-steady state approximation

According to Fig. 2, in the last mechanism step, the active sites on the catalyst are liberated and become available for further reaction cycles. In this sense, the active sites and the concentrations of adsorbed species do not change in time [3,31]. Considering a purely reactive system (without convection or diffusion), the mass balances of non-adsorbed species and active sites, in one dimension, can be written as:

$$\frac{dC_A}{dt} = -k_1C_A\Psi+k_{-1}C_{AZ}$$

$$\frac{dC_B}{dt} = -k_2C_B\Psi^2$$

$$\frac{dC_C}{dt} = k_3C_{AZ}C_{BZ}-k_{-3}C_C\Psi^2$$

$$\frac{d\Psi}{dt} = k_3 C_{AZ} C_{BZ} - k_{-3} C_C \Psi^2$$

For reactive complex AZ and BZ, there is no temporal change according to the pseudo-steady state approximation:

$$\frac{dC_{AZ}}{dt} = \frac{dC_{BZ}}{dt} = 0$$

After solving the above algebraic equations, expressions for the concentration of adsorbed species C_{AZ} and C_{BZ} are obtained:

$$C_{AZ} = \frac{k_1 C_A C_B - k_2 C_B}{k_{-1}} ; C_{BZ} = \frac{k_1 C_A C_B - k_{-1} C_{AZ}}{k_3 C_{AZ}}$$

Fig. 3 compares the chemical species' dynamic behaviors when pseudo-steady approximation (that is, ZA and ZB are constants) and non-steady sate (when all chemical species have temporal change) are considered. This comparison is made under isothermal and isobaric conditions ($T = 300\ K$).

According to Fig. 3(a), when a pseudo-steady state of adsorbed species is assumed, the amount of CO_2 produced during the chemical reaction is overestimated since such assumption implies that all adsorbed species react to produce CO_2. Moreover, as shown in Fig. 3(b), the concentration of active sites does not decrease as fast as in the non-steady approach; in the latter, the active sites do not completely regenerate since there is a temporal decay known as *catalyst loss of activity*. Such behavior is consistent with the theoretical and experimental data reported in [32], in which an alumina-supported platinum catalyst exhibits deactivation (also called catalyst aging) when considering a diffusion-reaction model during the carbon monoxide oxidation in an isothermal, integral reactor under controlled conditions.

(a)

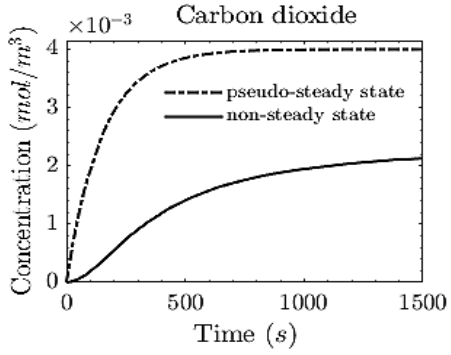

(b)

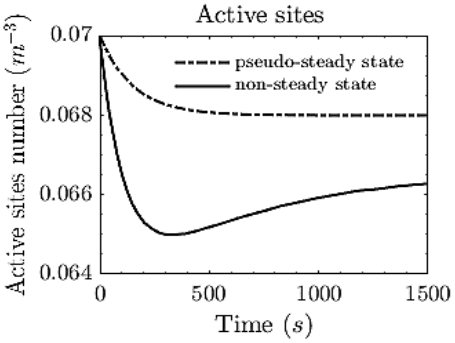

Figure 3. Concentration of chemical species comparing pseudo-steady state and non-steady state. (a) Molar concentration of CO_2 produced during the reaction. We compared the pseudo-steady (dashed line) and non-steady (solid line) assumptions. (b) Number of active sites per volume of catalyst. Under pseudo-steady state assumption, the number of active sites (dotted line) does not decrease faster than the non-steady profile.
Source: Own elaboration.

3.2 Non-isothermal reaction-diffusion system

In this case, Equations (6) and (7) are solved when the diffusion term $\partial^2 C_i / \partial x^2$ is non-zero, *i.e.*, we study a reaction-diffusion system under non-isothermal conditions. A staircase-type initial condition for the number of active sites per volume of catalyst (Ψ) was set up to observe diffusion within the gas phase [33].

$$f(x) = \begin{cases} \Psi_1 \ if \ 0 \leq x \leq 0.5 \\ \Psi_2 \ if \ 0.5 < x \leq 1 \end{cases}$$

were $\Psi_1 < \Psi_2$. The following figures show the spatial profile (the x-axis) of a specific variable (the y-axis) for each time step.

(a)

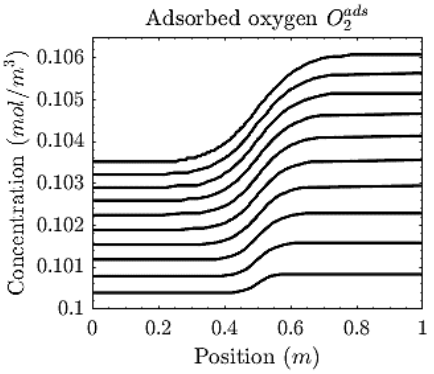

(b)

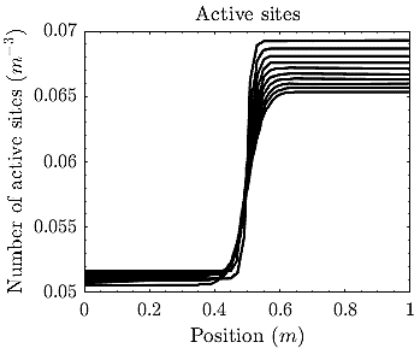

Figure 4. Concentration of chemical species for a non-isothermal reaction-diffusion system. (a) Molar concentration of adsorbed O_2. In each step, the adsorbed oxygen concentration increases since this reactant is adsorbed into the surface catalyst. (b) Number of active sites per volume of catalyst. When $0 \leq x \leq 0.5$, the number of active sites increases since the reactants are being adsorbed. Then, the available active sites decrease due to the incomplete desorption of the species.
Source: Own elaboration.

Fig. 4(a) shows the oxygen concentration in the gas phase, which temporarily decreases due to adsorption. It is worth noting that the transition due to the staircase-type initial conditions is smooth when the diffusion phenomenon is considered in the model. Additionally, the system's evolution is influenced mainly by the chemical reaction, and diffusion does not have a significant effect, at least from a macroscopic point of view. On the other hand, Fig. 4(b) shows the number of active sites per catalyst volume, which increases initially since the reactants are being adsorbed and immediately desorbed. In the end ($x > 0.5\ m$), contrary to what is expected, the available active sites decrease due to the incomplete desorption of the species, which shows the loss of activity of the catalyst.

Figs. 5(a) and (b) show the temperatures profiles in the gas phase and the catalyst, respectively. The adsorption steps of the chemical mechanism consume energy, and for this reason, the catalyst and gas temperatures decrease. Nonetheless, when the adsorbed species react, the temperature increases due to the exothermic nature of the reaction.

3.3 Catalyst deactivation

We consider two cases in which a catalyst could lose its activity, that is, deactivation by coking ($\nu_{poison} = 0$) and by poisoning ($\nu_{coke} = 0$).

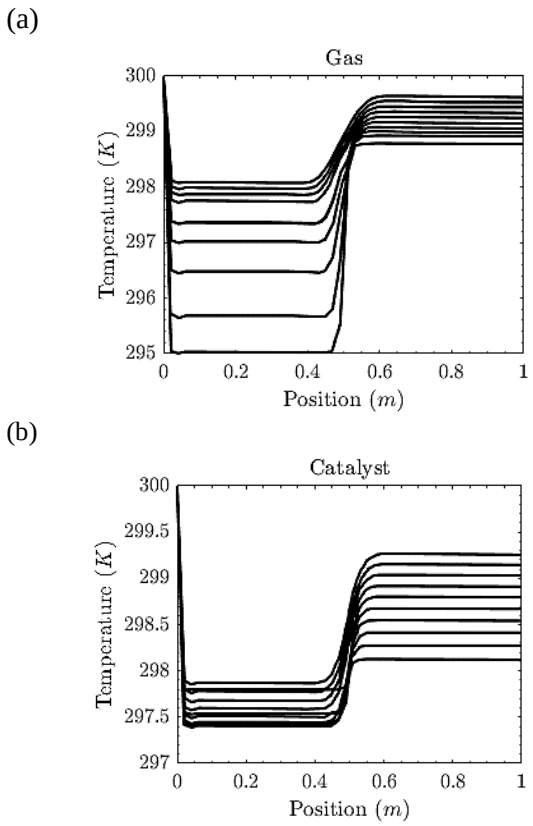

Figure 5. Temperature profiles for a non-isothermal reaction-diffusion system. (a) Gas temperature. When $0 \leq x \leq 0.5$, the gas temperature decreases because the reactants are adsorbed; however, the temperature increases due to the exothermic nature of the chemical reaction. (b) Catalyst temperature (surface). When $0 \leq x \leq 0.5$, the temperature decreases in every step of time. After that, the temperature increases because of the chemical reaction.
Source: Own elaboration.

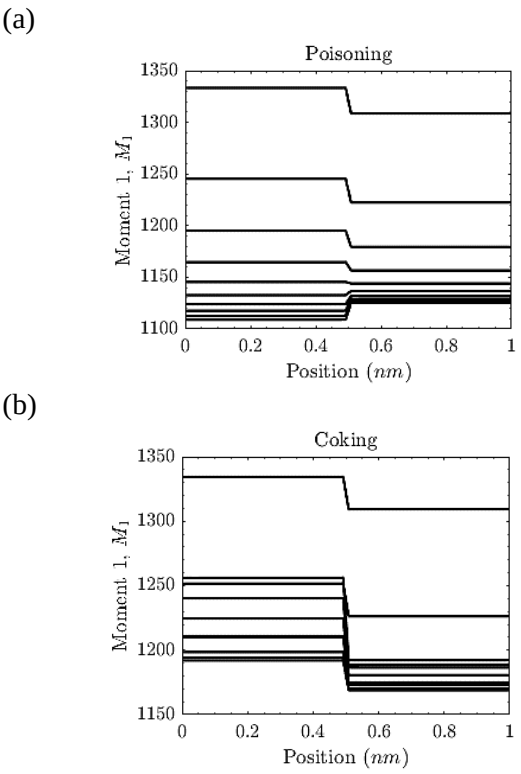

Figure 6. *Moment 1* - Catalyst deactivation. (a). Deactivation by poisoning. The total active area decreased from $1500\ m^2$ to $1150\ m^2$ at the end of the chemical reaction. (b). Deactivation by coking. The total active area decreased from $1500\ m^2\ to\ 1180\ m^2$ at the end of the chemical reaction.
Source: Own elaboration.

Fig. 6(a) and (b) show Moment 1 (which is related to the total active area) for poisoning and coking deactivation, respectively. From Fig. 7(a), the total active area decreases from $1500\ m^2$ (initial value) to $1150\ m^2$ approximately. In the case of deactivation by coking (Fig. 7(b)), the transition due to the staircase-like initial condition is more significant compared to the poisoning case. In other words, for each step of time, the average area of active sites has a significant decrease for $x > 0.5\ nm$.

Fig. 7 shows the active site area distribution, which is the average area of the population of active sites. In Fig. 7(a), the light colors indicate that, along the spatial coordinate, most of the active sites have an area between $1.10 - 1.15\ nm^2$ while the dark colors indicate that a small portion of the population of active sites has an area between $2.5 - 4.0\ nm^2$. In Fig. 7(b), the light colors indicate that, along the spatial coordinate, most of the active sites have an area between $1.18 - 1.20\ nm^2$ while the dark colors indicate that a small portion of the population of active sites has an area between $2.5 - 4.0\ nm^2$. The average area of active sites in both scenarios is statistically equal, so it is impossible to establish with certainty which mechanism has the most significant influence on the catalyst deactivation process.

4 Conclusions

In this work, we have implemented two complementary approaches: macroscopic balances and population balances,

to analyze a heterogenous catalysis reaction. When deriving the macroscopic balances of the system under consideration, we have proposed two different modeling domains with their respective equations set: one for the bulk fluid surrounding the catalyst cell without the catalytic reaction term, and one for the catalyst cell or interface system (see Fig. 1). Moreover, there is continuity in concentration and fluxes of chemical species within the subsystems' internal boundaries. We also have assumed the homogenized approximation at the macroscopic level [34], which is accurate given the relative size of the interface compared to the whole system. Additionally, since we have assumed a net adsorption-desorption rate across the y-axis, we can describe the macroscopic system with a 1D model along the system, from the inlet to the outlet. Thus, we obtained a model with two independent variables: position along the x-direction and time. A similar approach is implemented in [34].

Subsequently, we have studied and presented the results for a case study corresponding to the catalytic oxidation of carbon monoxide. For this case study, we have considered two scenarios: pseudo-steady state approximation and the more realistic case of a non-isothermal reaction-diffusion system.

(a)

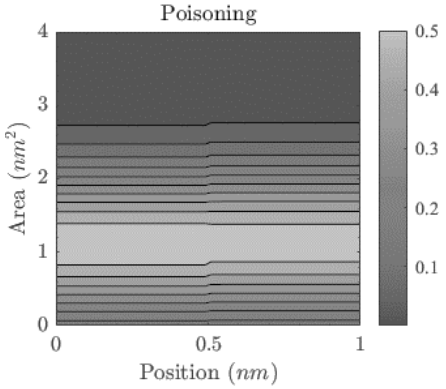

(b)

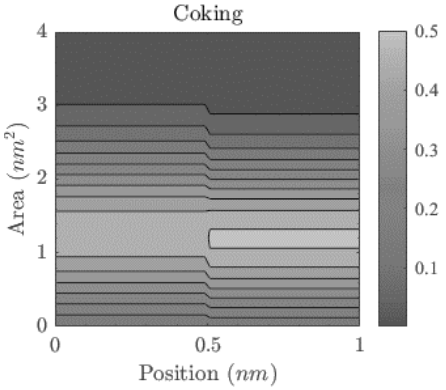

Figure 7. Active site area distribution. (a) Deactivation by poisoning. The light colors indicate that, along the spatial coordinate, most of the active sites have an area between $1.10 - 1.15\ nm^2$ while the dark colors indicate that a small portion of the population of active sites has an area between $2.5 - 4.0\ nm^2$. (b) Deactivation by coking. The light colors indicate that, along the spatial coordinate, most of the active sites have an area between $1.18 - 1.20\ nm^2$ while the dark colors indicate that a small portion of the population of active sites has an area between $2.5 - 4.0\ nm^2$.
Source: Own elaboration.

According to the simulation results, under the pseudo-steady state approximation and when the catalyst deactivation was not considered, the amount of product at the end of the chemical reaction is overestimated. This fact is consistent with the results reported in [32], and indicates that the temporal changes of the reactive complex have a significant influence on the reaction yield.

Additionally, the proposed formalism allows us to evaluate and determine which of all the considered transport phenomena has the most significant influence over the catalyst performance. For the application case of carbon monoxide oxidation (section 3), the system's evolution is not affected when diffusive phenomena are taken into account at the catalyst surface. In this sense, the system's evolution is mainly governed by chemical reaction, and the effect of the diffusion is just softening the transition according to the staircase type initial condition.

It is worth noting that, when facing the challenge of studying heterogeneous catalysis processes, software packages come in handy. For instance, COMSOL is an extensively used tool that implements models from the microscopic particle level to the macroscopic reactor level. Overall, the results we have reported are in accordance with the findings reported in [35,36], where the authors used COMSOL for heterogeneous catalysis under unsteady-state conditions [35], and in dynamic state at particle scale [36].

Finally, regarding the population balances, the average area of the active sites and the total active area of the catalyst decreases by coking and poisoning. However, it was not possible to determine the phenomenon that has a more significant influence during the catalyst deactivation process from the statistical information.

Nomenclature

x , y	Spatial coordinates
Z	Active site of the catalyst
C	Molar concentration (mol/m^3)
C_p	Heat capacity (J/K)
D	Diffusion coefficient (m^2/s)
$\bar{H}_i$	Partial molar enthalpy (J/mol)
J	Mass flux $(Kg/\ s\ m^2)$
L	System length (m)
N_i	Total molar flux (mol/m^2)
P	Pressure (Pa)
q	Heat transferred between phases (J)
R	Ideal gas constant $(J/mol\ K)$
T	Temperature (K)
t	Time (s)
U	Total thermal resistance (W/m^2K)
v	Mass-average velocity (m/s)
δ	Gas film height (m)
μ	Viscosity of the mixture $(Pa.s)$
ϑ	Net rate of formation by chemical reactions (mol/s)
ρ	Density of the mixture (kg/m^3)
τ_{ij}	Viscous stress
Ψ	Number of active sites per volume of catalyst

References

[1] Santillán, M., Chemical kinetics, stochastic processes, and irreversible thermodynamics. Springer International Publishing, New York, USA, 2014. DOI: https://doi.org/10.1007/978-3-319-06689-9.

[2] Hossain, M.M., Atanda, L., Al-Yassir, N. and Al-Khattaf, S., Kinetics modeling of ethylbenzene dehydrogenation to styrene over a mesoporous alumina supported iron catalyst. Chem. Eng. J. (207-208), pp. 308-321, 2012. DOI: https://doi.org/10.1016/j.cej.2012.06.108.

[3] Garayhi, A.R. and Keil, F.J., Modeling of microkinetics in heterogeneous catalysis by means of frequency response techniques. Chem. Eng. J., 82, pp. 329-346, 2001. DOI: https://doi.org/10.1016/S1385-8947(00)00364-8.

[4] Kozuch, S. and Shaik, S., Kinetic-Quantum chemical model for catalytic cycles: the Haber−Bosch process and the effect of reagent concentration. J. Phys. Chem. A., 112, pp. 6032-6041, 2008. DOI: https://doi.org/10.1021/jp8004772.

[5] Chumakov, G.A., Chumakova, N.A. and Lashina, E.A., Modeling the complex dynamics of heterogeneous catalytic reactions with fast, intermediate, and slow variables. Chem. Eng. J., 282, pp. 11-19, 2015. DOI: https://doi.org/10.1016/j.cej.2015.03.017.

[6] Rubi, J.M., Bedeaux, D., Kjelstrup, S. and Pagonabarraga, I., Chemical cycle kinetics: removing the limitation of linearity of a non-equilibrium thermodynamic description. Int. J. Thermophys., 34, pp. 1214-1228, 2015. DOI: https://doi.org/10.1007/s10765-013-1484-1.

[7] Schlexer, P., Computational Modeling in Heterogeneous Catalysis. Elsevier Inc., 2017. DOI: https://doi.org/10.1016/b978-0-12-409547-2.14273-8.

[8] Randolph, A.D. and Larson, M.A., Theory of Particulate Processes. Elsevier, 1971. DOI: https://doi.org/10.1016/B978-0-12-579650-7.X5001-5.

[9] Niemann, B. and Sundmacher, K., Reduced discrete population balance model for precipitation of barium sulfate nanoparticles in non-ionic microemulsions. Chem. Eng. J., 143, pp. 314-325, 2008. DOI: https://doi.org/10.1016/j.cej.2008.06.012.

[10] Verkoeijen, D., Pouw, G. A., Meesters, G.M.H. and Scarlett, B., Population balances for particulate processes - A volume approach. Chem. Eng. Sci., 57, pp. 2287-2303, 2002. DOI: https://doi.org/10.1016/S0009-2509(02)00118-5.

[11] Chorkendorff, I. and Niemantsverdriet, J.W., Concepts of Modern Catalysis and Kinetics. Wiley Ed., 2003. DOI: https://doi.org/10.1002/3527602658.

[12] Parmon, V.N., Catalysis and non-equilibrium thermodynamics: modern in situ studies and new theoretical approaches. Catal. Today. 51, pp. 435-456, 1999. DOI: https://doi.org/10.1016/S0920-5861(99)00032-2.

[13] Chattoraj, D.K. and Birdi, K.S., Adsorption and the Gibbs surface excess. Springer, Boston, MA, USA, 1984. DOI: https://doi.org/10.1007/978-1-4615-8333-2.

[14] Bedeaux, D., Kjelstrup, S., Zhu, L. and Koper, G.J.M., Nonequilibrium thermodynamics - A tool to describe heterogeneous catalysis. Phys. Chem. Chem. Phys., 8, pp. 5421-5427, 2006. DOI: https://doi.org/10.1039/B610041D.

[15] Zhu, L., Koper, G.J.M. and Bedeaux, D., Heats of transfer in the diffusion layer before the surface and the surface temperature for a catalytic hydrogen oxidation (H 2 + (1/2)O 2 → H 2 O) reaction. J. Phys. Chem. A., 110, pp. 4080-4088, 2006. DOI: https://doi.org/10.1021/jp056301i.

[16] Sha, M., Liu, Y., Dong, H., Luo, F., Jiang, F., Tang, Z., Zhu, G. and Wu, G., Origin of heterogeneous dynamics in local molecular structures of ionic liquids. Soft Matter. 12, pp. 8942-8949, 2016. DOI: https://doi.org/10.1039/c6sm01797e.

[17] Cruz, C., Barragán, D., Magnanelli, E., Lervik, A. and Kjelstrup, S., Non-equilibrium thermodynamics as a tool to compute temperature at the catalyst surface. Phys. Chem. Chem. Phys., 21, 2019. DOI: https://doi.org/10.1039/c9cp02389e.

[18] Bedeaux, D. and Kjelstrup, S., Heat, mass and charge transport, and chemical reactions at surfaces. Int. J. Thermodyn., 8, pp. 25-41, 2005.

[19] Bird, R.B., Stewart, W.E. and Lightfoot, E.N., Transport phenomena. Wiley, USA, 2007.

[20] Deen, W.M., Analysis of Transport Phenomena. Oxford University Press, UK, 1998.

[21] Barragán, D., Entropy production and Newton's cooling law. Ing. e Investig., 29, pp. 88-93, 2009. http://www.bdigital.unal.edu.co/19213/1/15167-45952-1-PB.pdf.

[22] Ramkrishna, D., Population balances. Elsevier, 2000. DOI: https://doi.org/10.1016/B978-0-12-576970-9.X5000-0.

[23] Hendriksen, B.L.M., Ackermann, M.D., van Rijn, R., Stoltz, D., Popa, I., Balmes, O., Resta, A., Wermeille, D., Felici, R., Ferrer, S. and Frenken, J.W.M., The role of steps in surface catalysis and reaction oscillations. Nat. Chem. 2, pp. 730-734, 2010. DOI: https://doi.org/10.1038/nchem.728.

[24] Vendelbo, S.B., Elkjær, C.F., Falsig, H., Puspitasari, I., Dona, P., Mele, L., Morana, B., Nelissen, B.J., Van Rijn, R., Creemer, J.F., Kooyman, P.J. and Helveg, S., Visualization of oscillatory behaviour of Pt nanoparticles catalysing CO oxidation. Nat. Mater., 13, pp. 884-890, 2014. DOI: https://doi.org/10.1038/nmat4033.

[25] Khazanchi, R., Reddy, D. c Bhatia, D., Kinetic model for the reversible deactivation of a Pt/Al_2O_3 catalyst during NO oxidation. Chem. Eng. J., 314, pp. 139-151, 2017. DOI: https://doi.org/10.1016/j.cej.2016.12.042.

[26] Ivanova, V., Baunach, T. and Kolb, D.M., Metal deposition onto a thiol-covered gold surface: a new approach. Electrochim. Acta. 50, pp. 4283-4288, 2005. DOI: https://doi.org/10.1016/j.electacta.2005.05.047.

[27] Rawlins, W.T. and Gardiner, W.C., Rate constant of OH + OH = H_2O + O from 1500 to 2000 K. J. Chem. Phys. 60, pp. 4676-4681, 1974. DOI: https://doi.org/10.1063/1.1680967.

[28] Marchisio, D.L., Pikturna, J.T., Fox, R.O., Vigil, R.D. and Barresi, A.A., Quadrature method of moments for population-balance equations. AIChE J., 49, pp. 1266-1276, 2003. DOI: https://doi.org/10.1002/aic.690490517.

[29] Dorao, C.A. and Jakobsen, H.A., Numerical calculation of the moments of the population balance equation. J. Comput. Appl. Math., 196, pp. 619-633, 2006. DOI: https://doi.org/10.1016/j.cam.2005.10.015.

[30] Dorao, C.A. and Jakobsen, H.A., The quadrature method of moments and its relationship with the method of weighted residuals. Chem. Eng. Sci., 61, pp. 7795-7804, 2006. DOI: https://doi.org/10.1016/j.ces.2006.09.014.

[31] Davis, M.E. and Davis, R.J., Fundamentals of Chemical Reaction Engineering, McGraw-Hill Higher Education , New York, USA, 2013.

[32] Hegedus, L.L., Oh, S.H. and Baron, K., Multiple steady states in an isothermal, integral reactor: The catalytic oxidation of carbon monoxide over platinum-alumina. AIChE J. 23, pp. 632–642, 1977. DOI: https://doi.org/10.1002/aic.690230503.

[33] Murray, J.D., Mathematical Biology. Springer New York, USA, 2002. DOI: https://doi.org/10.1007/b98868.

[34] Fontes, E., COMSOL: modeling approaches in heterogeneous catalysis, [online]. 2015. Available at: https://www.comsol.com/blogs.

[35] Pietrzyk, S., Dhainaut, F., Khodakov, A. and Granger, P., Catalytic Reactions under Unsteady-State Conditions. Modelling with COMSOL, COMSOL Users Conf. 2006, 2006.

[36] Patan, A.K., Mekala, M. and Thamida, S.K., Dynamic Simulation Using COMSOL Multiphysics for Heterogeneous Catalysis at Particle Scale. 2016.

C. Cruz, is a PhD. in Chemical Sciences with experience in modeling and simulation of multi-scale physical/chemical systems. She completed a five-year undergraduate program in Chemical Engineering and a two-year MSc. in Chemistry, both from the Universidad Nacional de Colombia, Medellin campus. In 2021, she completed a four-year PhD. program in Chemical Sciences at the Institute of Physical Chemistry in Warsaw, Poland, under the Marie Skłodowska-Curie grant. During her doctoral studies, Carolina joined the research group of Complex Systems and Chemical Processing of Information, where she studied the thermodynamic performance of ionic liquids in supercapacitors as promising sustainable energy storage devices. Currently, she is a postdoctoral researcher at the Chalmers University of Technology in Gothenburg, Sweden. She is a member of Patrik Johansson's Research Group, where she works on the computational modeling of next-generation batteries.
ORCID: 0000-0002-6319-0740

D. Barragán, is associate professor at the Escuela de Química, Facultad de Ciencias at the Universidad Nacional de Colombia, Medellin campus. Is BSc. in Chemist and Dr. in Chemistry, 2003. Research and teaching interests in non-equilibrium thermodynamics, nonlinear chemical dynamics, and physical chemistry.
ORCID: 0000-0002-7390-1104